Wide Angle X-Ray Diffraction Evidence of Structural Coherence in $CsPbBr_3$ Nanocrystal Superlattices

Stefano Toso,[†] Dmitry Baranov,[†*] Cinzia Giannini,[‡*] Sergio Marras,[†] Liberato Manna[†*]

[†]Nanochemistry Department, Istituto Italiano di Tecnologia, Via Morego 30, 16163 Genova, Italy

[‡]Istituto di Cristallografia (IC-CNR), via Amendola 122/O, I-70126 Bari, Italy

*E-mail: dmitry.baranov@iit.it, cinzia.giannini@ic.cnr.it, liberato.manna@iit.it

Contents:

S1. Materials and methods

a) Synthesis of $CsPbBr_3$ nanocrystals (NCs)

The $CsPbBr_3$ NCs used in this work have been synthesized following the hot-injection method developed by Protesescu et al.[1] with optimized amounts of oleic acid and oleylamine as developed by Almeida et al.[2] The list of reagents and detailed synthetic steps to produce NCs are described in a prior publication.[3] Briefly, the $CsPbBr_3$ NCs were synthesized by injecting a cesium oleate solution in octadecene-1 into a solution of lead (II) bromide dissolved in a mixture of oleylamine and oleic acid in octadecene-1. The injection was performed at ~160-165 °C.

b) Isolation of $CsPbBr_3$ NCs and preparation of the stock solution for self-assembly

The outcome of the synthesis is a mixture of $CsPbBr_3$ NCs, octadecene-1, ligands, and reaction by-products. Once the reaction mixture cooled down to within ~10 degrees of the room temperature, the reaction vial was centrifuged for 3 minutes at 6000 rpm, yielding a bright green precipitate at the bottom of the vial and a clear, bright green supernatant. The supernatant was discarded. The vial was centrifuged again (3 min at 6000 rpm) to discard any remaining liquid. For that centrifugation step, the vials were oriented in the centrifuge such that the precipitate was pointing outwards, so the remaining liquid could be collected in the lower and opposite part of the vial. After the centrifugation, the residual liquid was removed from the NC solid and the walls of the vial by gentle tapping with an absorbing paper tissue.

Next, the remaining solid was dissolved in 200 µL of tetrachloroethylene (TCE) and transferred in a 4 ml vial. The liquid at this stage looks turbid. The sample was centrifuged again for 3 min at 6000 rpm, the supernatant was recovered and filtered with a syringe filter (Sartorius, Minisart® SRP4, part no. 17820----------K, 0.45 µm pore size, hydrophobic PTFE) to eliminate any residual aggregates. The resulting sample is a clear bright-green stock solution of $CsPbBr_3$ NCs.

The suitability of the sample for growing NC superlattices (SLs) was checked by measuring the photoluminescence (PL) spectrum of a dilute solution of NCs. NC batches were deemed suitable for self-assembly experiments when the full width at half maximum of the emission spectra was <80 meV.[3] The solution for PL and absorbance measurements was prepared by diluting 6 µL of the NC solution (measured with a 10 µL mechanical micropipette) in 2994 µL of toluene (measured with a 1000 µL mechanical micropipette) in a quartz cuvette. The toluene was used for dilution instead of TCE. The PL spectra were measured in 90 degrees geometry using a Cary Eclipse spectrofluorimeter, λ_{exc} = 350 nm. The absorbance spectra were recorded using a Cary 500 UV-Vis spectrophotometer and corrected for the extinction spectrum of toluene solvent. The concentration of stock solution of NCs in TCE was adjusted by adding extra volume of TCE such that the absorbance of the dilute sample (6 μL of NCs in TCE + 2994 μL of toluene) at 335 nm was 0.50±0.05 or 0.30±0.05, in order to obtain films of densely-packed NC SLs or isolated SLs, respectively.

c) Self-assembly experiments on top of silicon substrates

The self-assembly was set up in a glass Petri dish using monocrystalline Si substrates. The Si substrates were cleaned by rinsing with toluene and isopropanol and dried by blowing compressed air. Three 1 cm x 1 cm Si substrates (Ted Pella, Inc., 10 x 10 mm diced Silicon Wafer, 55 chips/wafer, <100> orientation, catalog number 16006) were placed approximately equidistantly from each other with a polished side up inside a glass Petri dish (inner dimensions are 49 mm diameter by 13 mm height). The Petri dish was then set on top of a flat and leveled lab jack inside the ventilated fume hood. The surface of the lab jack was leveled with a spirit level. 30 μl of the stock solution of NCs TCE (prepared as explained in the preceding section) were deposited on each Si substrate, ensuring that the solution completely covers the surface without spilling underneath the wafer. The Petri dish was covered with a matching glass lid and left undisturbed overnight. The three silicon substrates were used per each assembly experiment for two main reasons: 1) to have a sufficiently high volume (~90 μl) of TCE inside the Petri dish to keep the evaporation process slow and 2) to produce replicas of the NC SLs for characterizations.

For the monitoring of SLs growth *in situ* by X-ray diffraction (XRD), the samples were prepared in a way similar as described above, except the custom-designed 3D-printed chamber covered with X-ray transparent Kapton (8 μm thick film) was used in place of the glass Petri dish. The chamber was printed using an Anet-A8 custom-built 3D printer and was made of polylactic acid polymer. The polymer was found to be resistant to TCE by an overnight immersion test in pure TCE (no degradation of the 3D-printed part was observed upon visual and tactile inspection). The *.stl files for the 3D-printed chamber are available online.[4]

d) Transmission electron microscopy (TEM) and fast Fourier transform (FFT) analysis of the images

The samples were prepared for TEM experiments by drop-casting a dilute solution of NCs onto a carbon-coated copper grid. The TEM images were collecting with a JEOL JEM-1011 electron microscope. The TEM images (*.dm3 file format) were processed using Digital Micrograph™ software version 1.71.38. The fast Fourier transforms (FFTs) of the TEM images were obtained by using Process -> FFT tool on a square region of interest (ROI). The periodicity was extracted from FFTs by measuring intensity profiles of the line ROIs passing through the center of the FFT and the centers of the bright spots, followed by the measuring the distance between peaks (as illustrated in Figures S10-S12). The reported spacing for each image is an average value obtained from 2-4 line profiles.

e) XRD experiments

XRD patterns were recorded using either Rigaku or PANalytical diffractometers. The Rigaku station was used for the in-plane and out-of-plane θ/2θ coupled measurements on the SL samples (Figure 1a,b in the main text), and *in situ* vacuum series (Figure 3 in the main text, Figure S13). For the *in situ* vacuum series, a domed stage (Anton Paar, DHS 900) connected to the rotary vacuum pump was used. The PANalytical station was used for out-of-plane XRD of randomly-oriented NCs (Figure 1c in the main text), out-of-plane XRDs (Figures S3, S14, S15), and *in situ* SLs growth observations (Figure 4 in the main text).

The Rigaku SmartLab X-ray powder diffractometer is equipped with a 9 kW CuKα rotating anode and five-axis goniometer, operating at 40 kV and 150 mA. A Göbel mirror was used to convert the divergent X-ray beam into a parallel beam and to suppress the Cu Kβ radiation.

The PANalytical Empyrean X-ray diffractometer is equipped with a 1.8kW CuKα ceramic X-ray tube, PIXcel^{3D} 2x2 area detector and operating at 45 kV and 40 mA. The diffraction patterns were collected in the air at room temperature using parallel-beam geometry and symmetric reflection mode.

Instrumental parameters for in-plane measurements (Rigaku):

Incident slit (IS): 0.1 mm
Receiver slits (RS1 and RS2): 20 mm
Parallel slit collimator (PSC): 0.5 degrees
Parallel slit analyzer (PSA): 0.5 degrees
Omega (incident beam angle): 0.4 degrees

Instrumental parameters for out-of-plane measurements (Rigaku):

IS, RS1, RS2: 1 mm
Soller slits: 5.0 degrees

Instrumental parameters for out-of-plane measurements (PANalytical):

Divergence fixed slit: 025 mm
Fixed mask: 2 mm
Soller slits: 2.3 degrees
Anti-scatter slits, incident beam: 1.4 mm (mirror)
Anti-scatter slits, receiver: 16.8 mm

S2. Satellite peaks at 2θ ~30.5° in XRD from $CsPbBr_3$ NC SLs

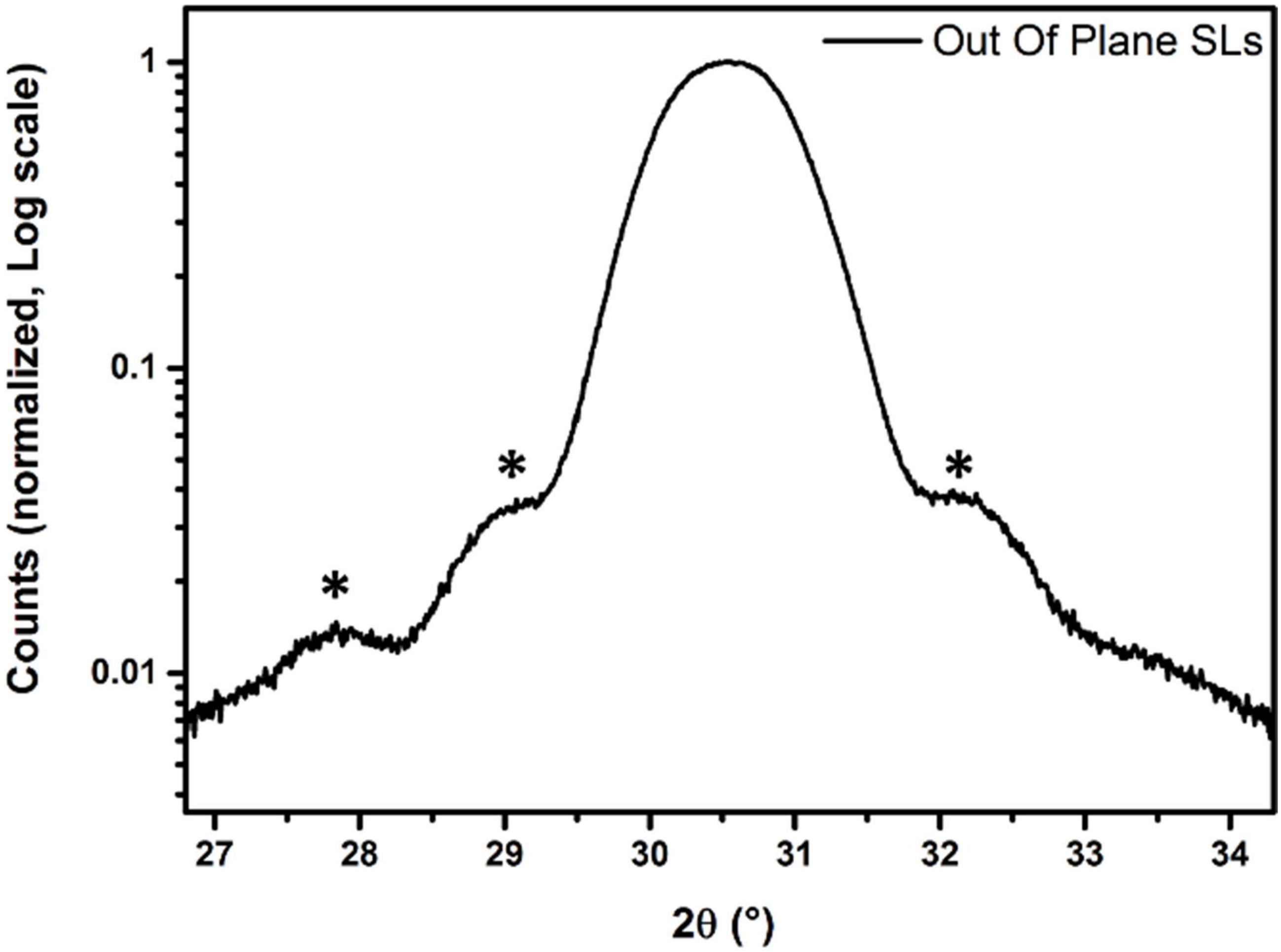

Figure S1. The satellite peaks (indicated by asterisks) at around 2θ ~30.5° peak in the XRD pattern of densely-packed $CsPbBr_3$ NC SLs. The figure reproduces the portion of data shown in Figure 1a in the main text plotted in logarithmic scale vs. scattering angle.

S3. Rietveld refinement of the powder XRD pattern of randomly-oriented $CsPbBr_3$ NCs

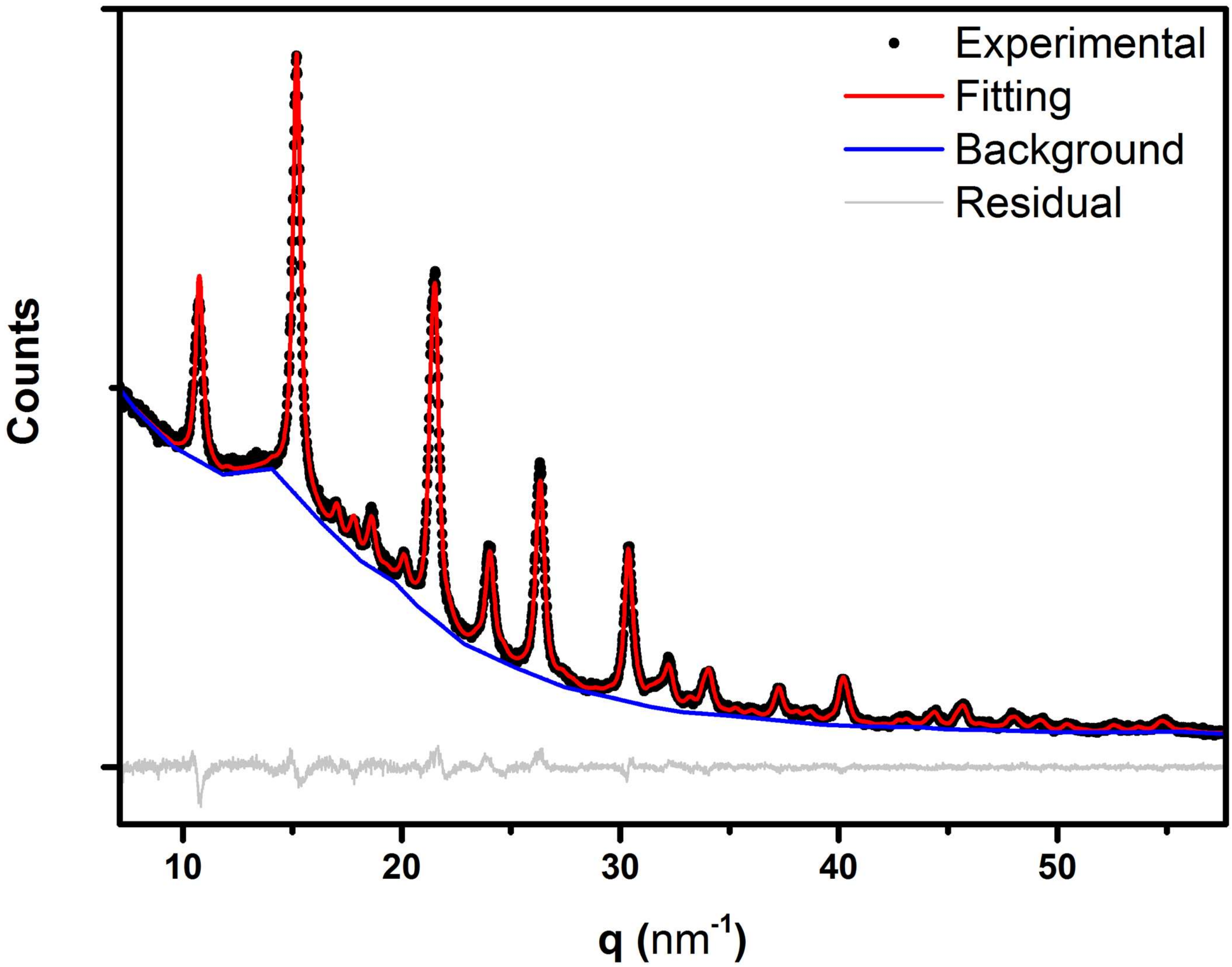

Figure S2. Rietveld refinement of the XRD pattern of randomly oriented NCs (Figure 1c in the main text), performed for refining the cell parameters. The sample was prepared by mixing a concentrated solution of $CsPbBr_3$ NCs in hexane with a powder of amorphous silica and depositing it on top of a zero-diffraction silicon wafer. Table S1 summarizes the Rietveld refinement results. Table S3 (page 18) provides an extended list of reflections from Rietveld refinement.

Table S1. Rietveld refinement results.

Space group	Pbnm (no. 62)
a, Å	8.2248
b, Å	8.2741
c, Å	11.7748
Z	4
volume, $Å^3$	801.1838
density calc, g/cm^3	4.807
Cs (x,y,z)	0.99000, 0.97100, 0.25000
Pb (x,y,z)	0.50000, 0, 0
Br1 (x,y,z)	0.04600, 0.50500, 0.25000
Br2 (x,y,z)	0.79300, 0.20500, 0.02500
B(Cs), $Å^2$	5.08
B(Pb), $Å^2$	1.07
B(Br1), $Å^2$	2.13
B(Br2), $Å^2$	2.19
G.O.F	1.5
Rp	10.7
Rwp	9.83
Re	6.53
Chi2	2.264

S4. Satellite peaks in XRD pattern from a sample of isolated $CsPbBr_3$ NC SLs

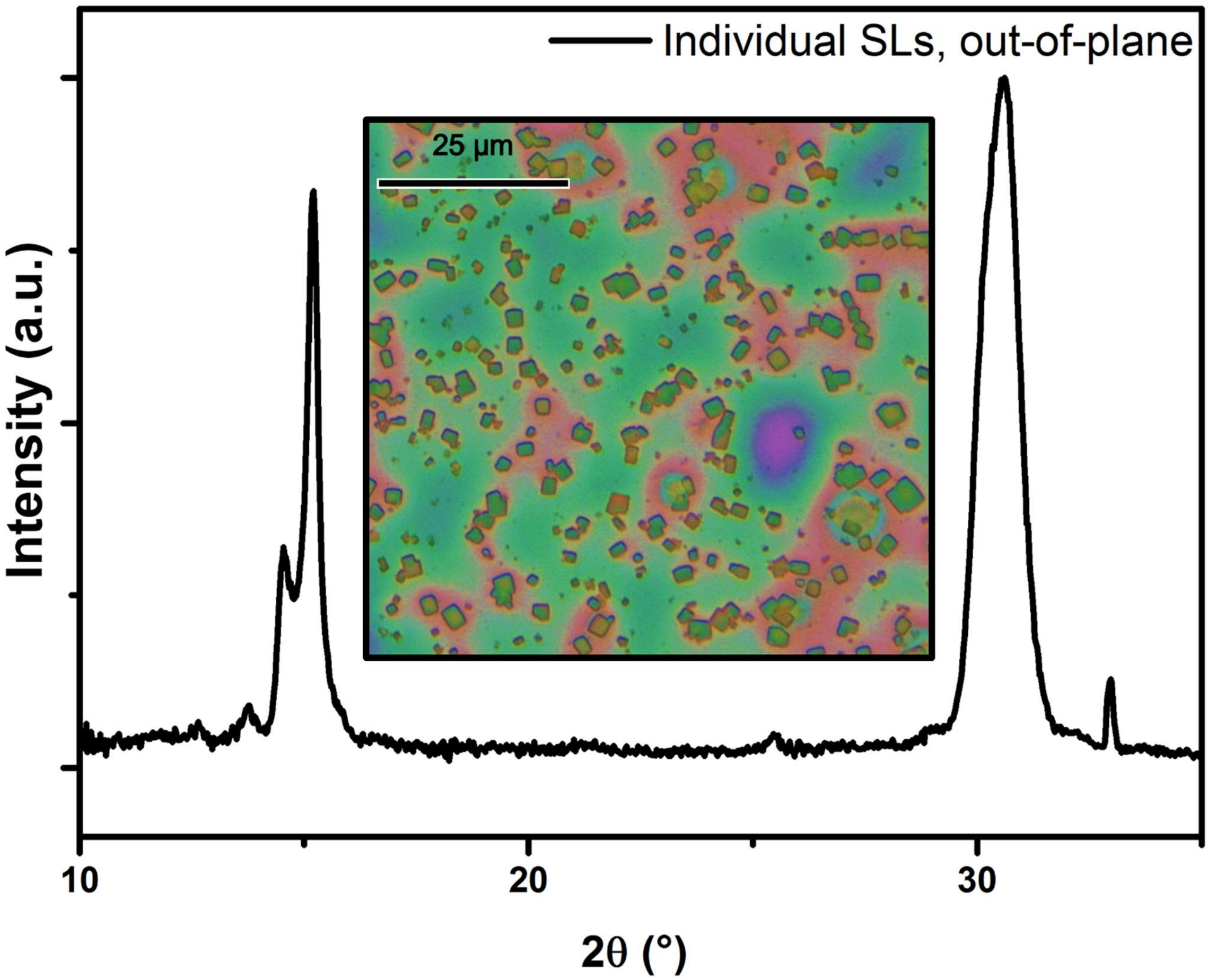

Figure S3. Out-of-plane XRD pattern from a sample of isolated $CsPbBr_3$ NC SLs (inset shows an optical microscopy image of the same sample). The prominent satellite peaks are visible in the region of the 2θ ~15° peak and weak satellites are observable in the region of the 2θ ~30.5° peak. The sharp peak at around 2θ ~33° is from Si substrate.[5]

S5. Optical and scanning electron microscopy images of the samples of $CsPbBr_3$ NC SLs

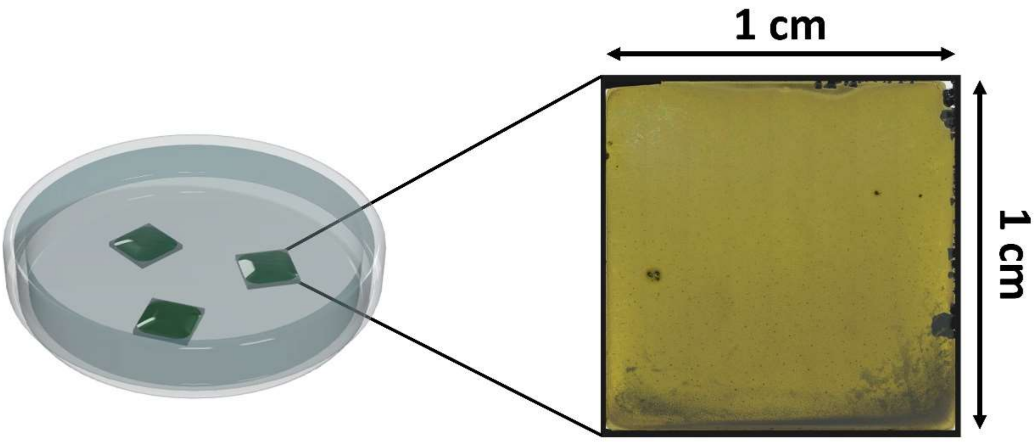

Figure S4. Self-assembly setup in a Petri dish (left panel) and an optical microscopy image of the entire Si substrate (right panel) covered with densely-packed $CsPbBr_3$ NC SLs after the self-assembly.

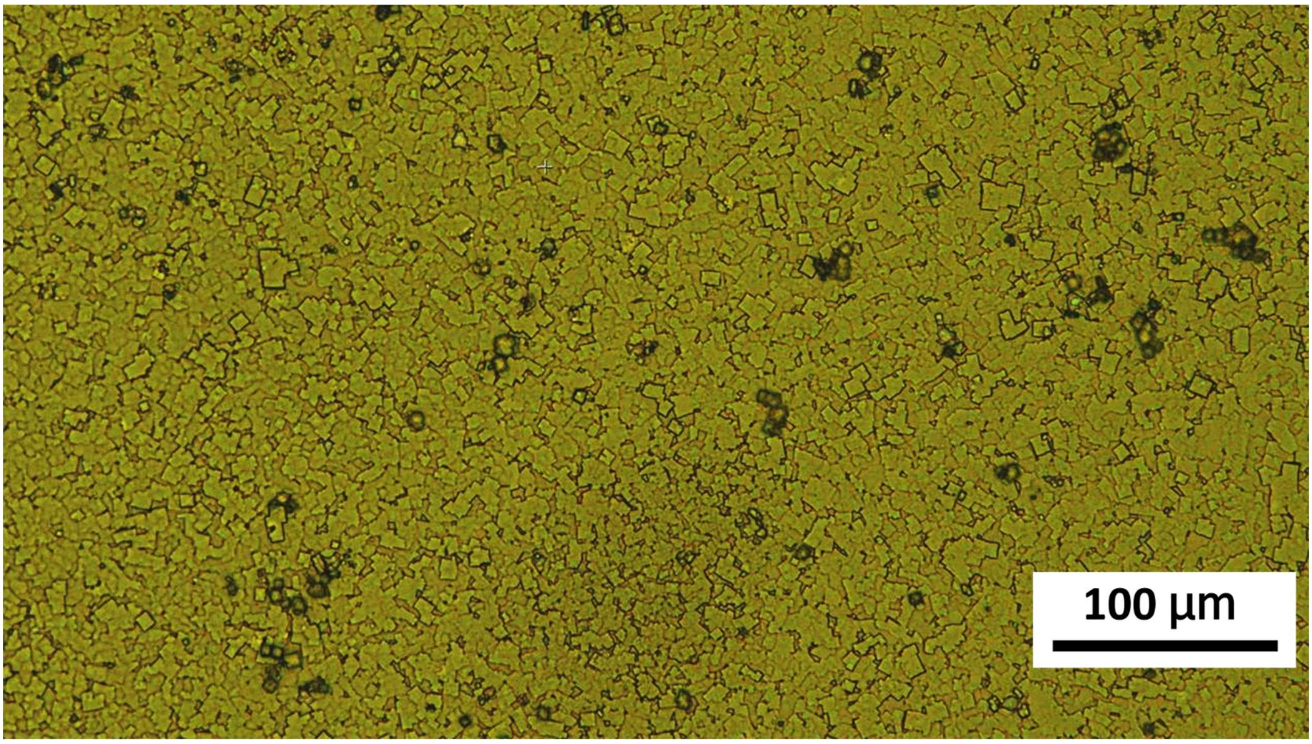

Figure S5. Optical microscopy image of the sample of densely-packed $CsPbBr_3$ NC SLs. The polygonal shapes of the "grains" with several right or nearly right angles are noticeable. The shapes of "grains" are similar to the isolated SLs. Typically, the coverage of the Si substrate with densely-packed SLs is homogeneous over several mm^2.

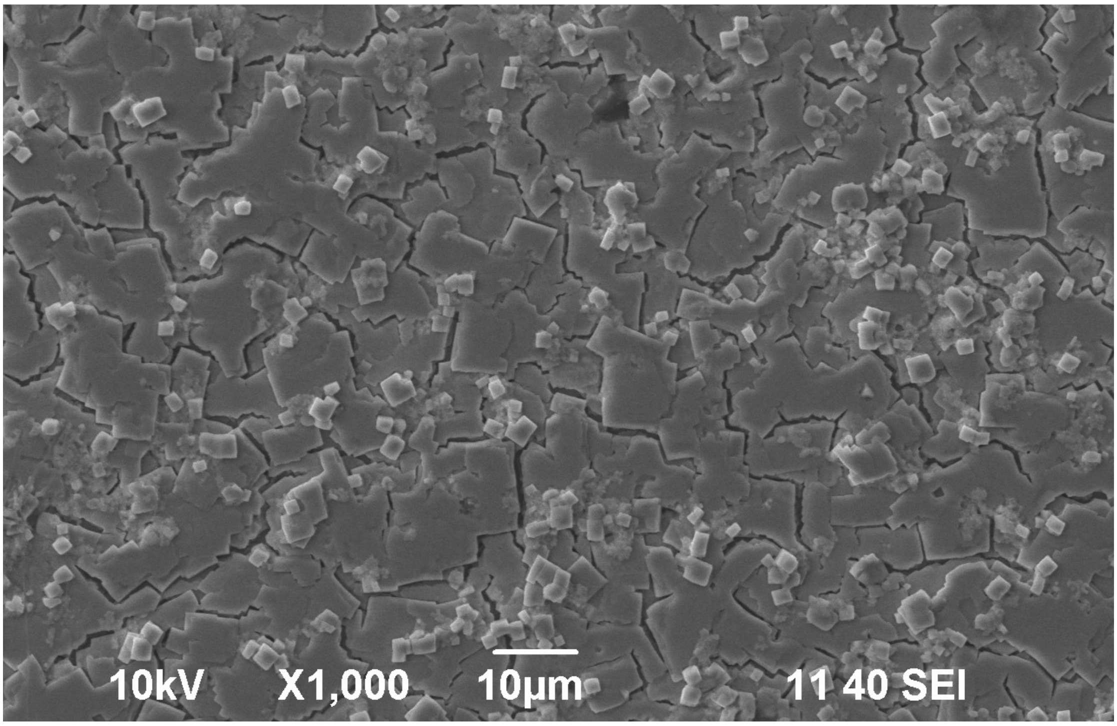

Figure S6. Scanning electron microscopy image of a sample of densely-packed $CsPbBr_3$ NC SLs.

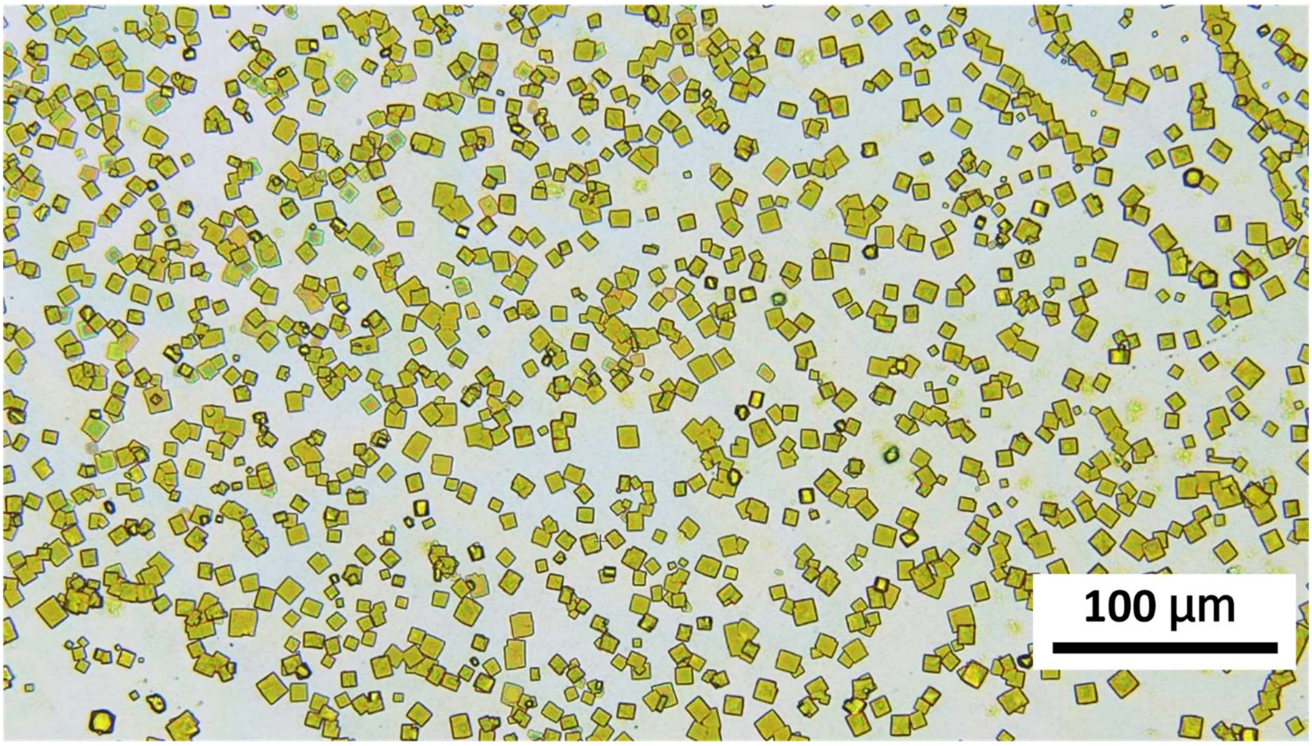

Figure S7. Optical microscopy image of the sample with isolated $CsPbBr_3$ NC SLs.

S6. Fits of the satellite peaks at 2θ ~15° in the XRD pattern of $CsPbBr_3$ NC SLs

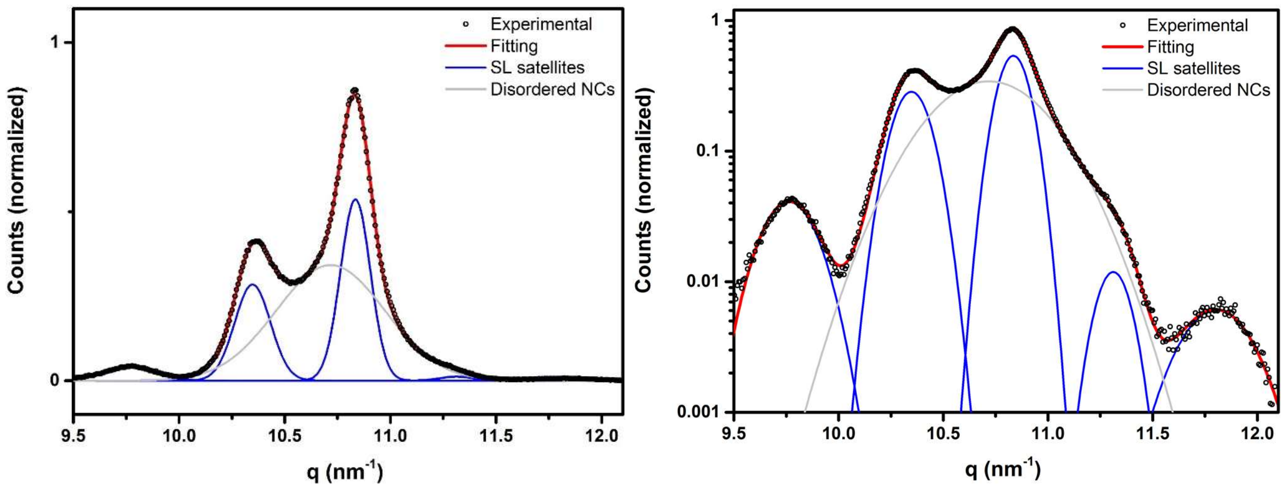

Figure S8. Fits of satellite peaks at 2θ ~15° in XRD from the film of densely-packed $CsPbBr_3$ NC SLs. The figure shows data from Figure 2 of the main text on the linear (left panel) and logarithmic (right panel) scales vs. scattering vector, q, nm^{-1}. The Gaussian fits of the satellite peaks are shown by blue lines; the peak from Bragg reflection of NCs is shown in grey. Table S2 summarizes the fit parameters.

Table S2. Fitting results. The best-fit parameters were obtained by minimizing the absolute difference between the fit and experimental data in Excel.

Peak	q_c, *nm*$^{-1}$	σ, *nm*$^{-1}$	*FWHM, nm*$^{-1}$	*A*
1, SL satellite	9.76236	0.12285	0.28929	0.022265
2, SL satellite	10.3481	0.08452	0.19903	0.106810
3, Bragg	10.7173	0.25727	0.60583	0.390374
4, SL satellite	10.8349	0.07065	0.16637	0.168413
5, SL satellite	11.3119	0.07642	0.17995	0.004007
6, SL satellite	11.8046	0.15966	0.37598	0.004285

Peak function, $I(q) = A\frac{1}{\sigma\pi\sqrt{2}}\exp(-\frac{(q-q_c)^2}{2\sigma^2})$;

Background, $I(q) = aq^2 + bq +$;

$a = 0.000515061, b = -0.0142375, c = -0.101933$

S7. Periodicity in close-packed $CsPbBr_3$ NCs from FFTs of TEM images

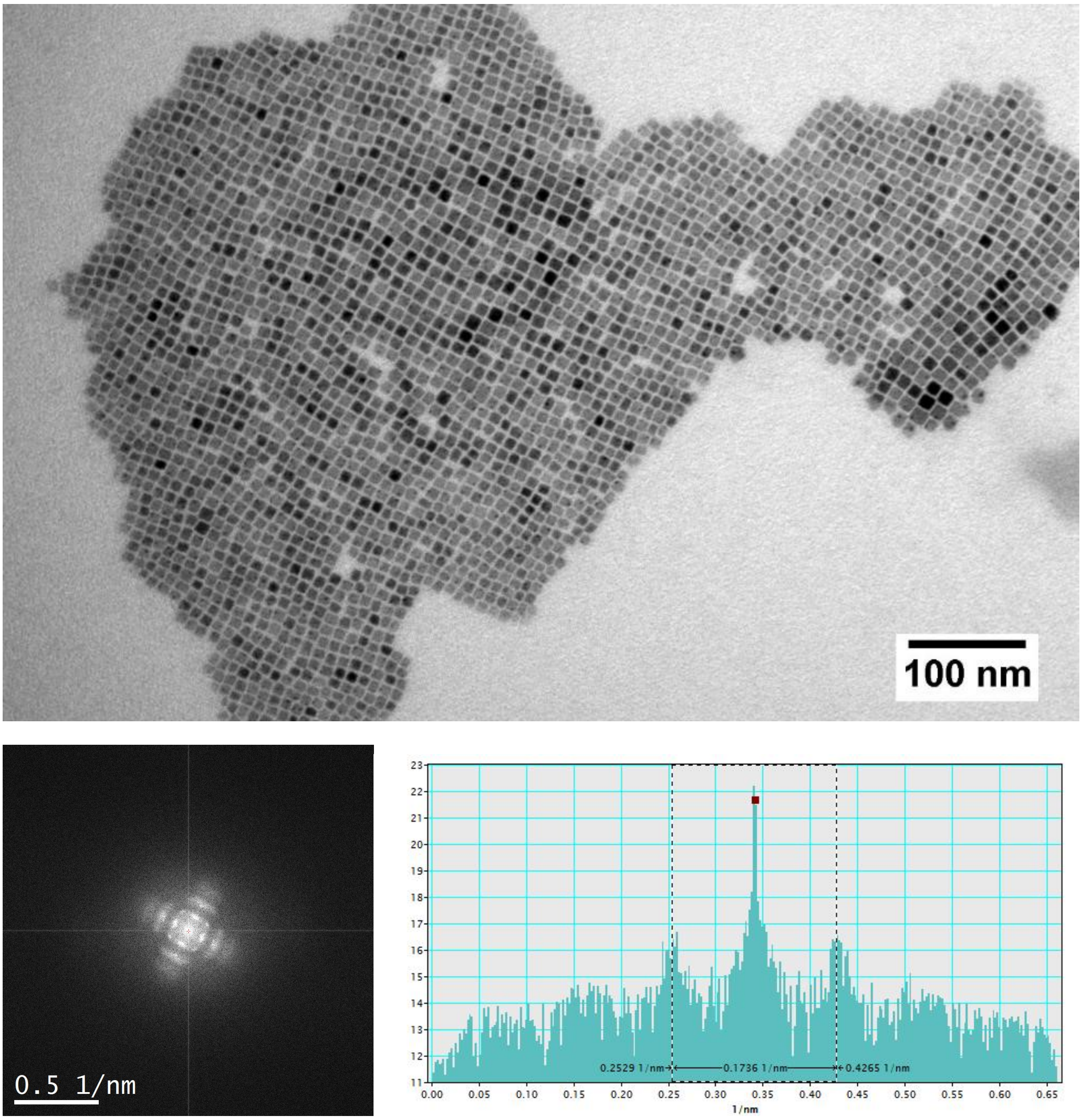

Figure S9. The TEM image of a close-packed monolayer of $CsPbBr_3$ NCs (top image), corresponding FFT pattern (lower left image), and one of the radial line profiles of the FFT pattern (vertical axis: intensity, a.u.; horizontal axis: 1/nm). The periodicity measured for this image is ~11.5 nm.

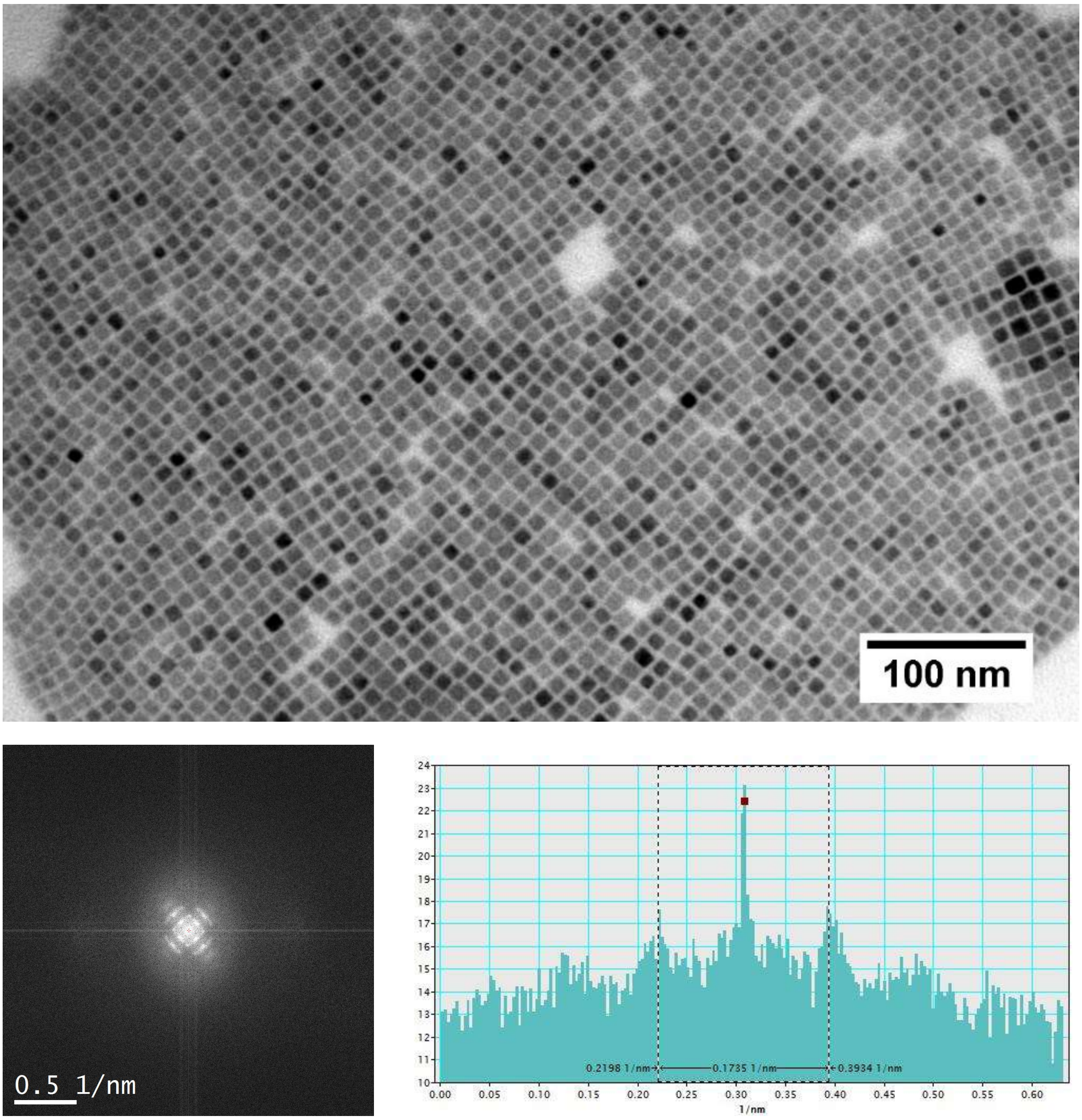

Figure S10. The TEM image of a close-packed monolayer of $CsPbBr_3$ NCs (top image), corresponding FFT pattern (lower left image), and one of the radial line profiles of the FFT pattern (vertical axis: intensity, a.u.; horizontal axis: 1/nm). The periodicity measured for this image is ~11.5 nm.

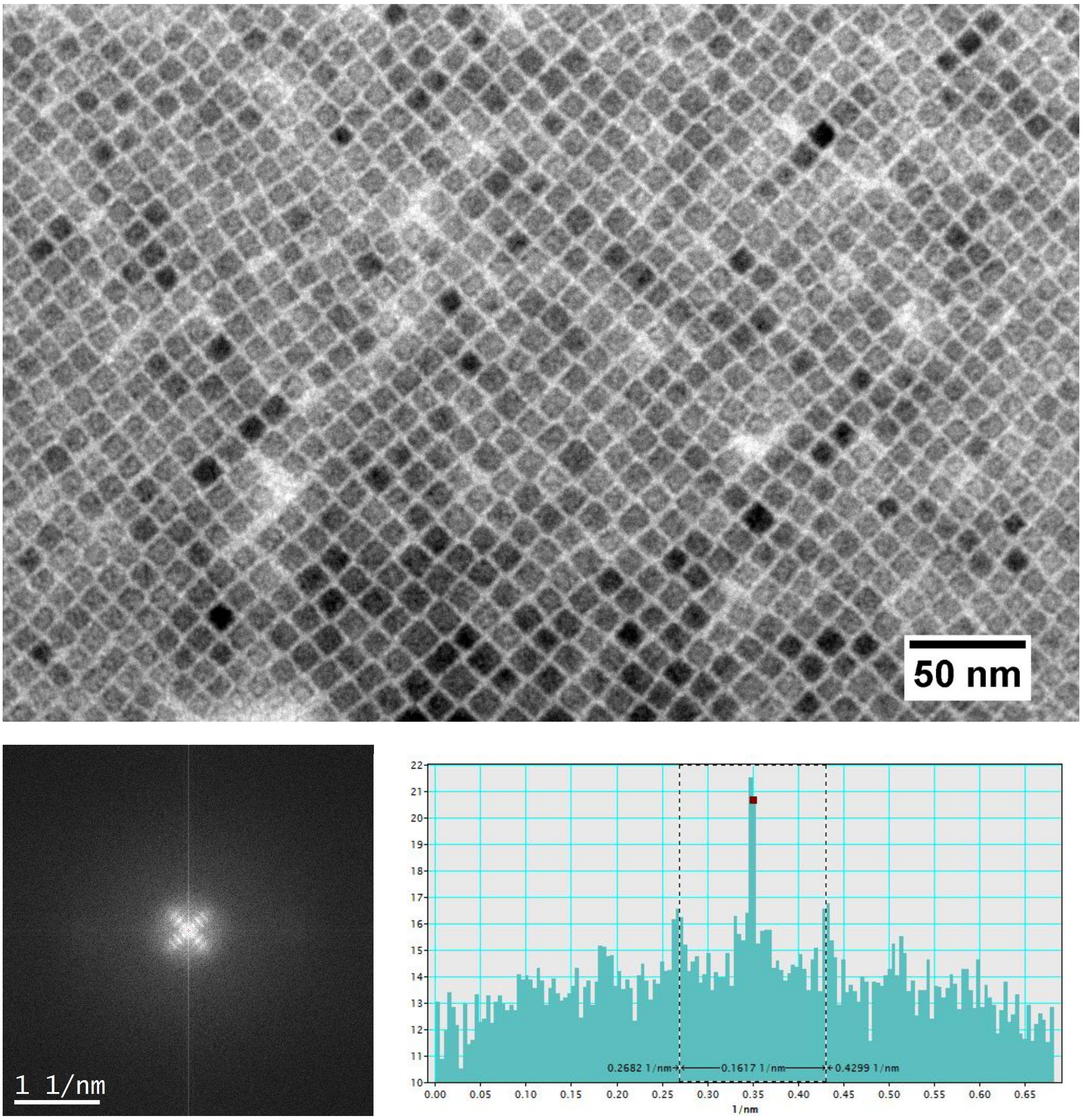

Figure S11. The TEM image of a close-packed monolayer of $CsPbBr_3$ NCs (top image), corresponding FFT pattern (lower left image), and one of the radial line profiles of the FFT pattern (vertical axis: intensity, a.u.; horizontal axis: 1/nm). The periodicity measured for this image is ~12.5 nm.

S8. SL wavelength contraction under vacuum

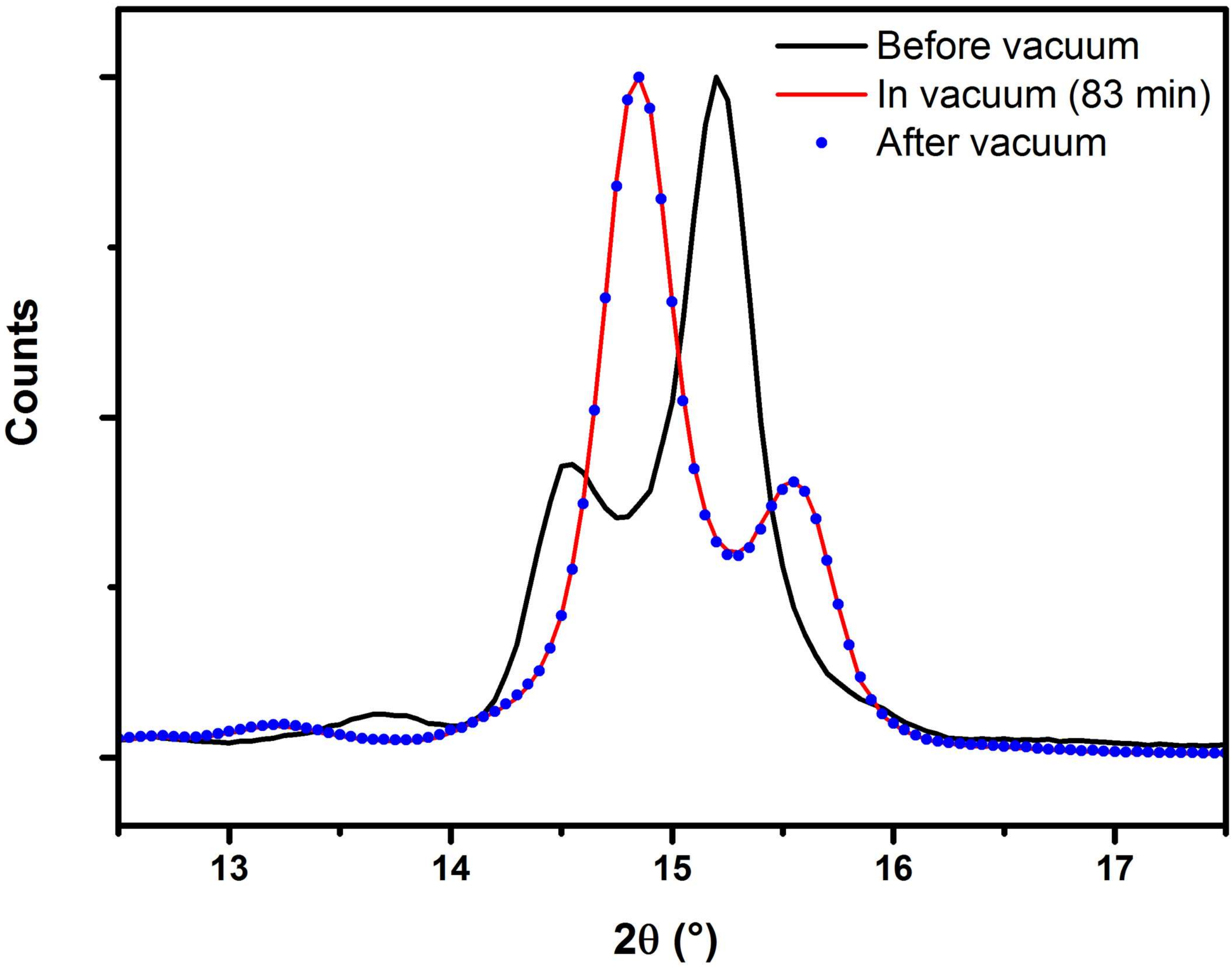

Figure S12. XRD patterns of the SL sample subjected to the vacuum experiment (Figure 3) showing XRD patterns at the start of the experiment (black line), at the end under vacuum (red line), and upon return to the ambient pressure (blue dots).

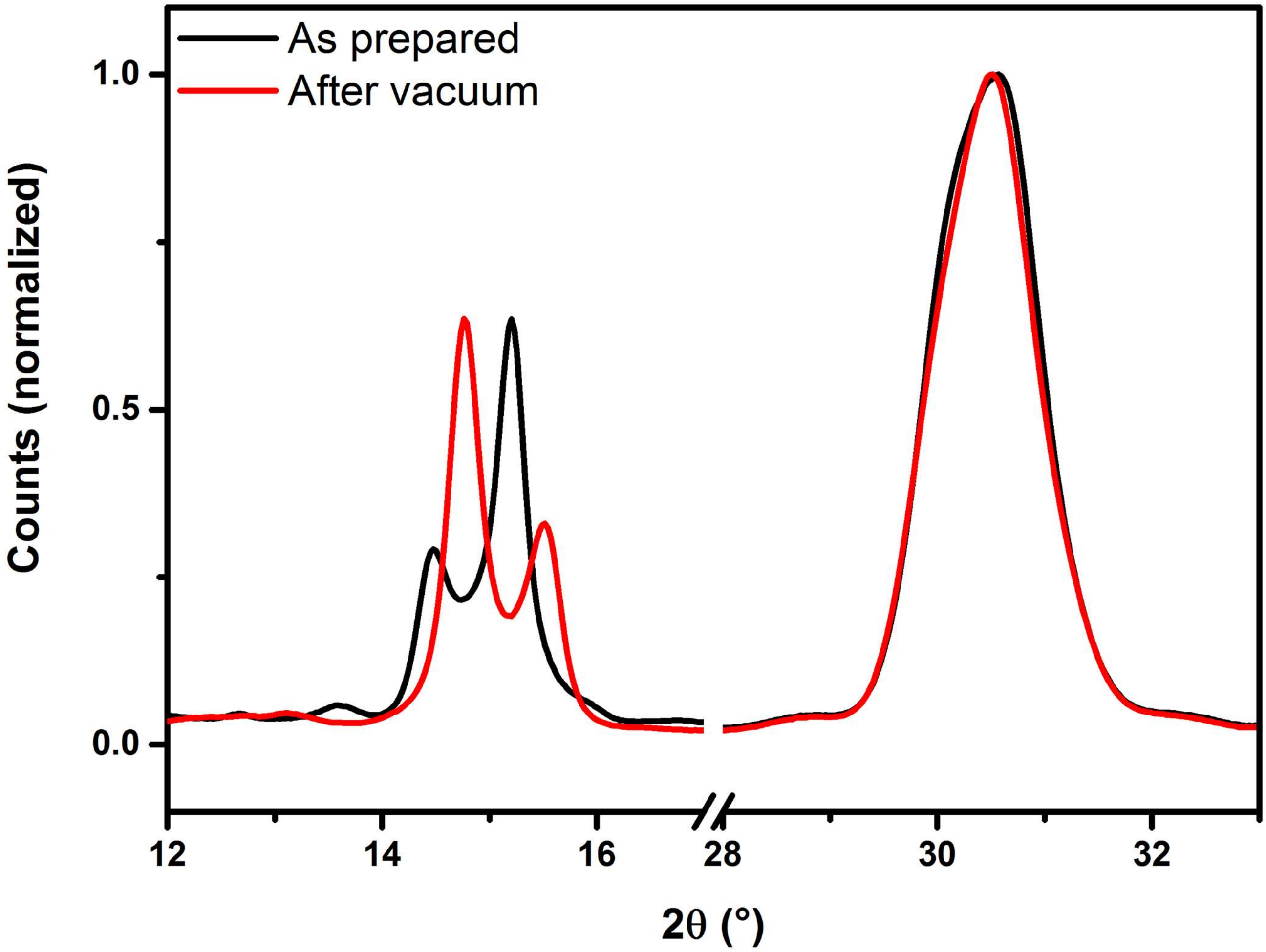

Figure S13. XRD patterns of another sample (sample 2, different from the one discussed in the main text) of $CsPbBr_3$ NC SLs before and after application of vacuum. The SL wavelength, Λ contracts from ~12.24 nm to ~12.00 nm (based on the fits, as described in the main text and Section S6 above).

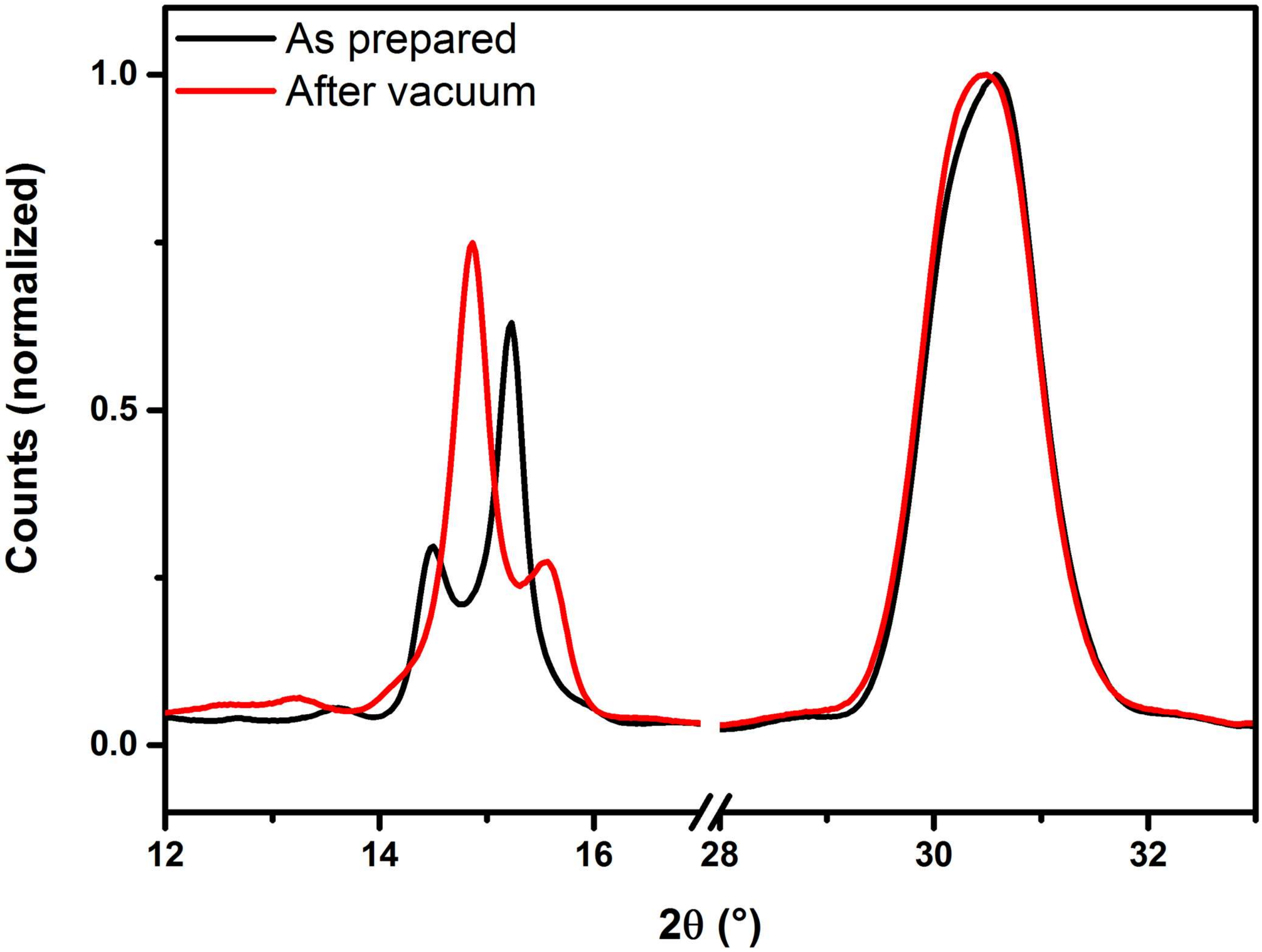

Figure S14. XRD patterns of another sample (sample 3, different from the one discussed in the main text) of $CsPbBr_3$ NC SLs before and after application of vacuum. The SL wavelength, *Λ* contracts from ~12.22 nm to ~11.94 nm (based on the fits, as described in the main text and Section S6 above).

S9. An extended list of reflections from the Rietveld refinement

Table S3. An extended list of reflections used in the Rietveld refinement.

2θ, degrees	*d-hkl, Å*	*Intensity (a.u., calc)*	*h*	*k*	*l*
13.119	6.74274	12	1	0	1
15.036	5.8874	947.1	0	0	2
15.176	5.83317	1716.7	1	1	0
16.949	5.22694	52.7	1	1	1
21.426	4.14371	4213.1	1	1	2
21.461	4.13705	1320.9	0	2	0
21.591	4.1124	1218	2	0	0
22.764	3.90315	22.8	0	2	1
24.059	3.69585	191.7	1	2	0
24.147	3.68262	185.7	2	1	0
25.119	3.54227	200.1	1	0	3
25.235	3.52623	70.7	1	2	1
25.319	3.51473	206.8	2	1	1
26.307	3.38491	384.8	0	2	2
26.415	3.37137	356.9	2	0	2
27.365	3.2564	77	1	1	3
28.491	3.13019	256.2	1	2	2
28.566	3.12214	217.9	2	1	2
30.338	2.9437	2114.4	0	0	4
30.627	2.91658	3566.4	2	2	0
31.391	2.84738	78.7	0	2	3
31.577	2.83103	64.3	2	2	1
33.27	2.6907	42.1	1	2	3
33.335	2.68559	51.2	2	1	3
33.533	2.67018	35.6	3	0	1
34.088	2.62802	494.4	1	1	4
34.264	2.61493	454.2	1	3	0
34.283	2.61347	381	2	2	2
34.433	2.60246	302.5	3	1	0
35.125	2.55274	96.2	1	3	1
35.291	2.54113	28.9	3	1	1
37.465	2.39849	589.1	0	2	4
37.544	2.39366	553.8	2	0	4
37.606	2.38981	957.5	1	3	2
37.763	2.38028	1244.8	3	1	2
38.421	2.34101	0.5	2	2	3
39.088	2.30258	50.5	1	2	4
39.145	2.29937	50.1	2	1	4
39.301	2.29059	20.8	2	3	0
39.395	2.28533	30.7	3	2	0

Table S3 (continued)					
2θ, degrees	*d-hkl, Å*	*Intensity (a.u., calc)*	***h***	***k***	***l***
39.782	2.26398	52	1	0	5
40.069	2.24844	24.6	2	3	1
40.085	2.24758	0.6	3	0	3
40.161	2.24347	8.5	3	2	1
41.31	2.18371	0.5	1	1	5
41.459	2.17619	27.8	1	3	3
41.603	2.16898	8.7	3	1	3
42.303	2.13471	22.5	2	3	2
42.392	2.13045	19	3	2	2
43.651	2.07186	1853	2	2	4
43.725	2.06853	398.9	0	4	0
44.001	2.0562	361.5	4	0	0
44.218	2.04661	3	0	2	5
44.43	2.03733	28.2	0	4	1
45.161	2.00606	78.6	1	4	0
45.413	1.9955	67.8	4	1	0
45.641	1.98605	82.2	1	2	5
45.691	1.98398	37.3	2	1	5
45.829	1.97833	47.4	2	3	3
45.848	1.97756	0.4	1	4	1
45.912	1.97494	48.8	3	2	3
46.097	1.96745	58.5	4	1	1
46.221	1.96247	23.2	0	0	6
46.408	1.95498	323.6	1	3	4
46.494	1.95157	44.4	0	4	2
46.54	1.94975	224.6	3	1	4
46.676	1.94439	24.2	3	3	0
46.757	1.94121	69.2	4	0	2
47.347	1.91841	13.5	3	3	1
47.864	1.89885	89.9	1	4	2
48.106	1.8899	89.6	4	1	2
48.928	1.86002	286.8	1	1	6
49.27	1.84793	229	2	4	0
49.316	1.8463	145.4	3	3	2
49.459	1.84131	193.4	4	2	0
49.72	1.83225	34.8	2	2	5
49.787	1.82994	0.4	0	4	3
49.914	1.82558	8.4	2	4	1
50.101	1.8192	3.7	4	2	1
50.44	1.80777	9.9	2	3	4
50.517	1.80518	15.5	3	2	4
51.086	1.7864	31.2	3	0	5

Table S3 (continued)					
2θ, degrees	***d-hkl, Å***	***Intensity (a.u., calc)***	***h***	***k***	***l***
51.09	1.78627	9.8	1	4	3
51.32	1.7788	57.5	4	1	3
51.498	1.77309	3.3	0	2	6
51.559	1.77113	2.3	2	0	6
51.811	1.76311	1.6	2	4	2
51.993	1.75737	4.1	4	2	2
52.231	1.74992	25.3	1	3	5
52.351	1.74617	37.6	3	1	5
52.476	1.74231	32.3	3	3	3
52.771	1.73327	10.2	1	2	6
52.816	1.7319	8.4	2	1	6
54.146	1.69246	306.2	0	4	4
54.381	1.68568	275	4	0	4
54.868	1.67189	40.8	2	4	3
55.043	1.66699	8	4	2	3
55.377	1.65772	43.1	1	4	4
55.594	1.65175	36.9	4	1	4
55.612	1.65125	9.4	3	4	0
55.714	1.64849	11.2	4	3	0
55.732	1.648	34.7	1	0	7
55.954	1.64198	0.3	2	3	5
56.026	1.64004	1.4	3	2	5
56.205	1.63525	8.3	3	4	1
56.305	1.63257	34.1	4	3	1
56.434	1.62914	2.7	5	0	1
56.47	1.6282	46.8	2	2	6
56.689	1.62241	39	3	3	4
56.693	1.62231	51.4	1	5	0
56.925	1.61625	8.5	1	1	7
57.036	1.61338	12.2	5	1	0
57.278	1.60713	20.2	1	5	1
57.618	1.59845	0.1	5	1	1
57.957	1.5899	31.9	3	4	2
58.056	1.58743	21.5	4	3	2
58.779	1.56961	140.8	1	3	6
58.891	1.5669	182.8	3	1	6
58.966	1.5651	222.2	2	4	4
59.01	1.56402	63	1	5	2
59.133	1.56107	189.3	4	2	4
59.251	1.55823	12.2	0	2	7
59.344	1.55601	150.9	5	1	2
59.423	1.55413	26.3	0	4	5

Table S3 (continued)					
2θ, degrees	*d-hkl, Å*	*Intensity (a.u., calc)*	***h***	***k***	***l***
60.232	1.53519	0.1	2	5	0
60.414	1.531	19.4	1	2	7
60.455	1.53005	2.5	2	1	7
60.52	1.52856	0	5	2	0
60.584	1.5271	1.5	1	4	5
60.789	1.52243	9.2	4	1	5
60.795	1.52231	7.8	2	5	1
60.807	1.52204	1.4	3	4	3
60.902	1.51988	4	4	3	3
61.025	1.51711	4.2	5	0	3
61.082	1.51584	6.2	5	2	1
61.826	1.49937	0.1	3	3	5
61.83	1.49929	14.3	1	5	3
62.155	1.49223	12.4	5	1	3
62.244	1.4903	1.6	2	3	6
62.311	1.48885	1	3	2	6
62.467	1.48552	0.4	2	5	2
62.749	1.47951	1.8	5	2	2
63.113	1.47185	81.7	0	0	8
63.769	1.45829	98.8	4	4	0
63.825	1.45714	2.2	2	2	7
63.99	1.45378	2.1	2	4	5
64.15	1.45055	0	4	2	5
64.314	1.44723	6.4	4	4	1
64.669	1.44015	5.4	3	4	4
64.762	1.43831	7.1	4	3	4
64.993	1.43376	2	3	0	7
65.199	1.42972	0.3	2	5	3
65.332	1.42712	61.8	1	1	8
65.475	1.42436	2.2	5	2	3
65.509	1.42369	10	0	4	6
65.658	1.42083	61.9	1	5	4
65.719	1.41965	15.6	4	0	6
65.871	1.41674	75.7	3	5	0
65.936	1.41551	34.4	4	4	2
65.972	1.41482	18.7	5	1	4
65.979	1.41469	1.1	1	3	7
66.084	1.41271	8.5	3	1	7
66.081	1.41277	51.5	5	3	0
66.408	1.4066	8.3	3	5	1
66.609	1.40283	7	1	4	6
66.616	1.4027	4.7	5	3	1

Table S3 (continued)					
2θ, degrees	*d-hkl, Å*	*Intensity (a.u., calc)*	*h*	*k*	*l*
66.804	1.39921	7.4	4	1	6
67.487	1.3867	72.2	0	2	8
67.539	1.38577	68.7	2	0	8
67.79	1.38124	47.5	3	3	6
67.914	1.37902	38.6	0	6	0
68.003	1.37742	130.5	3	5	2
68.209	1.37377	179.6	5	3	2
68.377	1.3708	26	6	0	0
68.442	1.36966	0.9	0	6	1
68.571	1.36741	0.5	1	2	8
68.595	1.36699	0.6	4	4	3
68.609	1.36673	0.6	2	1	8
68.927	1.3612	0.1	2	5	4
68.995	1.36003	10.6	1	6	0
69.196	1.35657	0	5	2	4
69.241	1.3558	11.8	2	3	7
69.305	1.35471	16.7	3	2	7
69.442	1.35237	11.2	6	1	0
69.463	1.35201	6.7	3	4	5
69.519	1.35105	0.3	1	6	1
69.552	1.35049	27.4	4	3	5
69.667	1.34855	0.4	5	0	5
69.856	1.34535	4.6	2	4	6
69.965	1.34353	13.3	6	1	1
70.009	1.34279	7	4	2	6
70.016	1.34268	8.6	0	6	2
70.418	1.33598	5.4	1	5	5
70.473	1.33509	14.1	6	0	2
70.625	1.33259	4.2	3	5	3
70.722	1.33099	7.5	5	1	5
70.827	1.32928	0.1	5	3	3
71.082	1.32514	21	1	6	2
71.523	1.31804	19	6	1	2
71.776	1.31401	147.2	2	2	8
72.192	1.30747	43	2	6	0
72.239	1.30673	103.2	4	4	4
72.346	1.30507	2.8	0	4	7
72.593	1.30123	33.7	6	2	0
72.605	1.30105	6.9	0	6	3
72.706	1.29948	5.5	2	6	1
73.106	1.29336	0.6	6	2	1
73.191	1.29207	6.9	1	0	9

Table S3 (continued)					
2θ, degrees	***d-hkl, Å***	***Intensity (a.u., calc)***	***h***	***k***	***l***
73.382	1.28918	0.3	4	5	0
73.397	1.28894	4.5	1	4	7
73.494	1.28749	1.3	5	4	0
73.584	1.28613	12.3	4	1	7
73.589	1.28605	8.5	2	5	5
73.655	1.28507	0.6	1	6	3
73.818	1.28263	46.5	1	3	8
73.85	1.28215	4.3	5	2	5
73.893	1.28152	2.9	4	5	1
73.918	1.28115	34.6	3	1	8
74.005	1.27986	2.4	5	4	1
74.09	1.2786	5.7	6	1	3
74.226	1.27659	0.4	1	1	9
74.226	1.27659	77.7	3	5	4
74.241	1.27637	9.9	2	6	2
74.424	1.27368	52.7	5	3	4
74.53	1.27213	9.2	3	3	7
74.638	1.27056	20.5	6	2	2
75.128	1.26349	3.9	3	4	6
75.214	1.26225	2.3	4	3	6
75.418	1.25934	0.2	4	5	2
75.53	1.25776	0	5	4	2
76.054	1.25038	22.7	1	5	6
76.169	1.24878	43.1	0	6	4
76.267	1.24742	1.1	0	2	9
76.35	1.24628	48.8	5	1	6
76.52	1.24393	14.6	2	4	7
76.612	1.24267	29	6	0	4
76.667	1.24191	2.3	4	2	7
76.774	1.24045	0.1	2	6	3
76.819	1.23983	5.5	4	4	5
76.935	1.23825	0.2	2	3	8
76.996	1.23742	0.4	3	2	8
77.166	1.23512	0.5	6	2	3
77.202	1.23463	7.6	1	6	4
77.3	1.23332	12.3	1	2	9
77.337	1.23282	3.3	2	1	9
77.401	1.23195	5.1	3	6	0
77.631	1.22889	8.2	6	1	4
77.732	1.22754	3.6	6	3	0
77.903	1.22526	1.7	3	6	1
77.938	1.2248	12	4	5	3

Table S3 (continued)					
2θ, degrees	*d-hkl, Å*	*Intensity (a.u., calc)*	***h***	***k***	***l***
78.048	1.22335	2.5	5	4	3
78.233	1.22092	3.9	6	3	1
78.766	1.21399	3.6	3	5	5
78.961	1.21148	6.6	5	3	5
79.142	1.20917	0	2	5	6
79.397	1.20592	0.3	5	2	6
79.404	1.20583	3.1	3	6	2
79.732	1.2017	4.2	6	3	2
79.928	1.19925	39.3	0	4	8
80.122	1.19683	33.8	4	0	8
80.277	1.1949	52.3	2	6	4
80.374	1.19371	4.3	2	2	9
80.665	1.19014	40.1	6	2	4
80.676	1.19	0.8	0	6	5
80.947	1.1867	1.1	1	4	8
81.128	1.1845	0.8	4	1	8
81.44	1.18076	5.3	3	0	9
81.428	1.1809	0.2	4	5	4
81.537	1.1796	1.1	5	4	4
81.64	1.17837	0	3	4	7
81.715	1.17748	0.8	0	0	10
81.693	1.17774	0	1	6	5
81.724	1.17737	0	4	3	7
81.833	1.17608	1.6	5	0	7
81.889	1.17541	1	3	6	3
82.048	1.17354	18	3	3	8
82.115	1.17275	8.1	6	1	5
82.215	1.17158	10.3	6	3	3
82.307	1.1705	13.1	4	4	6
82.346	1.17004	2.3	1	3	9
82.35	1.16999	23.7	1	7	0
82.421	1.16917	0.2	7	0	1
82.443	1.16891	6.4	3	1	9
82.546	1.16772	2.5	1	5	7
82.639	1.16663	0.8	5	5	0
82.835	1.16437	8.6	5	1	7
82.845	1.16426	3.1	1	7	1
82.928	1.1633	6.9	7	1	0
83.133	1.16095	1.2	5	5	1
83.422	1.15766	0.4	7	1	1
83.729	1.1542	23.2	1	1	10
83.989	1.15129	46.7	2	4	8

Table S3 (continued)					
2θ, degrees	*d-hkl, Å*	*Intensity (a.u., calc)*	***h***	***k***	***l***
84.133	1.14969	40.6	4	2	8
84.223	1.14869	35.4	3	5	6
84.325	1.14755	20	1	7	2
84.415	1.14657	49.7	5	3	6
84.53	1.1453	19	4	6	0
84.613	1.14438	7.1	5	5	2
84.73	1.1431	7.9	2	6	5
84.77	1.14267	15.3	6	4	0
84.901	1.14124	54.3	7	1	2
85.022	1.13992	0.8	4	6	1
85.113	1.13893	0.2	6	2	5
85.262	1.13732	0.8	6	4	1
85.344	1.13644	4.3	3	6	4
85.379	1.13606	0	2	3	9
85.383	1.13602	0.2	2	7	0
85.439	1.13542	0.6	3	2	9
85.578	1.13393	0.2	2	5	7
85.667	1.13298	2.8	6	3	4
85.712	1.1325	1.7	0	2	10
85.76	1.13199	2	2	0	10
85.829	1.13125	0.4	5	2	7
85.87	1.13082	0.1	4	5	5
85.875	1.13077	0.4	2	7	1
85.922	1.13027	0	7	2	0
85.978	1.12968	0.9	5	4	5
86.108	1.1283	3.6	0	6	6
86.364	1.12562	0.7	7	0	3
86.414	1.1251	0.8	7	2	1
86.498	1.12422	12.2	4	6	2
86.539	1.12379	6.4	6	0	6
86.719	1.12192	0	1	2	10
86.737	1.12173	14.7	6	4	2
86.755	1.12155	0	2	1	10
86.785	1.12124	2.8	1	7	3
87.072	1.11828	1.4	5	5	3
87.115	1.11783	2.9	1	6	6
87.359	1.11534	0.9	7	1	3
87.349	1.11545	0.3	2	7	2
87.533	1.11357	2.5	6	1	6
87.887	1.11	0.5	7	2	2
88.316	1.10571	4.4	0	4	9
88.705	1.10187	0.1	4	4	7

Table S3 (continued)					
2θ, degrees	***d-hkl, Å***	***Intensity (a.u., calc)***	***h***	***k***	***l***
88.952	1.09944	2.1	4	6	3
89.025	1.09873	0	3	4	8
89.109	1.09791	0.2	4	3	8
89.191	1.09712	0.5	6	4	3
89.321	1.09585	0.5	1	4	9
89.5	1.09412	0.6	4	1	9
89.736	1.09186	2.7	2	2	10
89.763	1.0916	0.7	3	6	5
89.802	1.09123	1.1	2	7	3
89.923	1.09008	10.2	1	5	8
89.763	1.0916	0.7	3	6	5
89.802	1.09123	1.1	2	7	3
89.923	1.09008	10.2	1	5	8

S10. References

1. Protesescu, L.; Yakunin, S.; Bodnarchuk, M. I.; Krieg, F.; Caputo, R.; Hendon, C. H.; Yang, R. X.; Walsh, A.; Kovalenko, M. V., Nanocrystals of Cesium Lead Halide Perovskites ($CsPbX_3$, X = Cl, Br, and I): Novel Optoelectronic Materials Showing Bright Emission with Wide Color Gamut. *Nano Lett.* **2015,** 15, (6), 3692-3696.

2. Almeida, G.; Goldoni, L.; Akkerman, Q.; Dang, Z.; Khan, A. H.; Marras, S.; Moreels, I.; Manna, L., Role of Acid–Base Equilibria in the Size, Shape, and Phase Control of Cesium Lead Bromide Nanocrystals. *ACS Nano* **2018,** 12, (2), 1704-1711.

3. Baranov, D.; Toso, S.; Imran, M.; Manna, L., Investigation into the Photoluminescence Red Shift in Cesium Lead Bromide Nanocrystal Superlattices. *J. Phys. Chem. Lett.* **2019**, 655-660.

4. Toso, S. Thingiverse Designs. https://www.thingiverse.com/tosostefanots/designs (June 11, 2019),

5. Zaumseil, P., High-resolution characterization of the forbidden Si 200 and Si 222 reflections. *J. Appl. Crystallogr.* **2015,** 48, (2), 528-532.